

Manganese oxides hierarchical structures derived from coordination polymers and their enhanced catalytic activity at low temperature for selective catalytic reduction of NO_x

Supporting Information.

Table of contents

Table S1. List of chemicals used for the synthesis of Mn-CP with their suppliers.

Fig. S1. FT-IR spectra of (a) sodium fumarate (b) Mn-CP.

Fig. S2. (a) Low- and (b) high-magnification FESEM images of the Mn-CP. (c - f) Elemental mapping data displaying the distribution of C, O and Mn in Mn-CP

Fig. S3. TGA curve of Mn-CP.

Fig. S4. (a) N₂ adsorption-desorption (BET isotherm) and (b) BJH pore size distribution of the MnO_x catalysts.

Fig. S5. (a) Low-magnification and (b) high-magnification FESEM images of MnO_x-350 after catalytic reaction for 10 hours.

Fig. S6. SEM images of MnO_x-300

Fig. S7. NO_x conversion efficiency of the MnO_x-300

Graphical abstract.

Chemicals	Suppliers
Pluronic F-127	Sigma-Aldrich
Potassium bromide	Sigma-Aldrich
Manganese(II) chloride tetrahydrate	Junsei Chemical Co., Ltd.
Disodium fumarate	Tokyo Chemical Industry Co., Ltd.
Acetone	Samchun Pure Chemical Co., Ltd.

Table S1. List of chemicals with their suppliers used for the synthesis of Mn-CP.

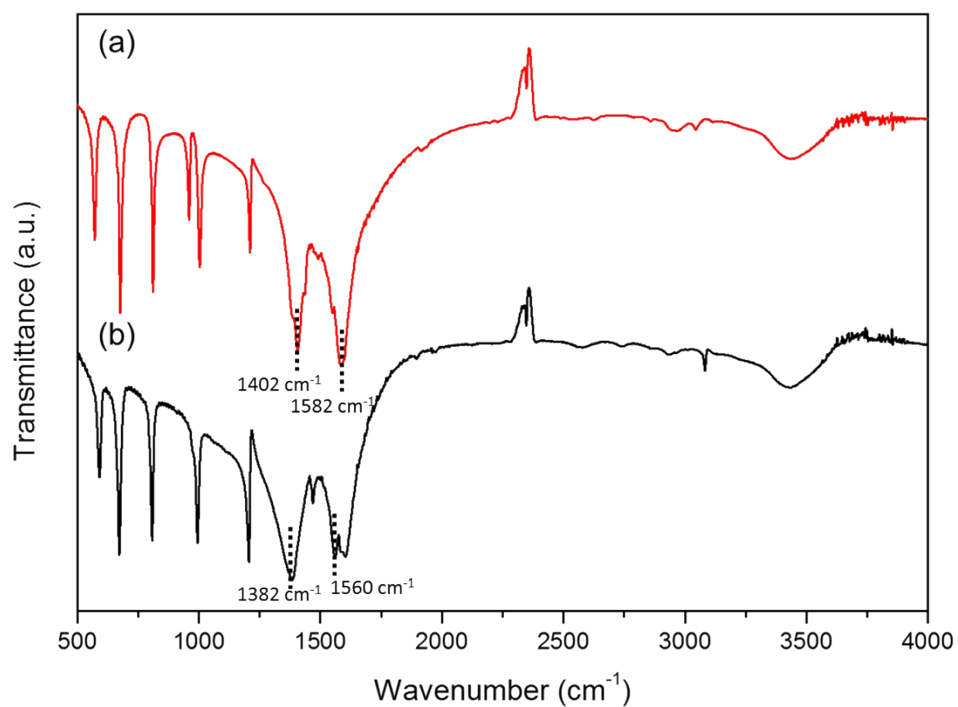


Fig. S1. FT-IR spectra of (a) sodium fumarate (b) Mn-CP.

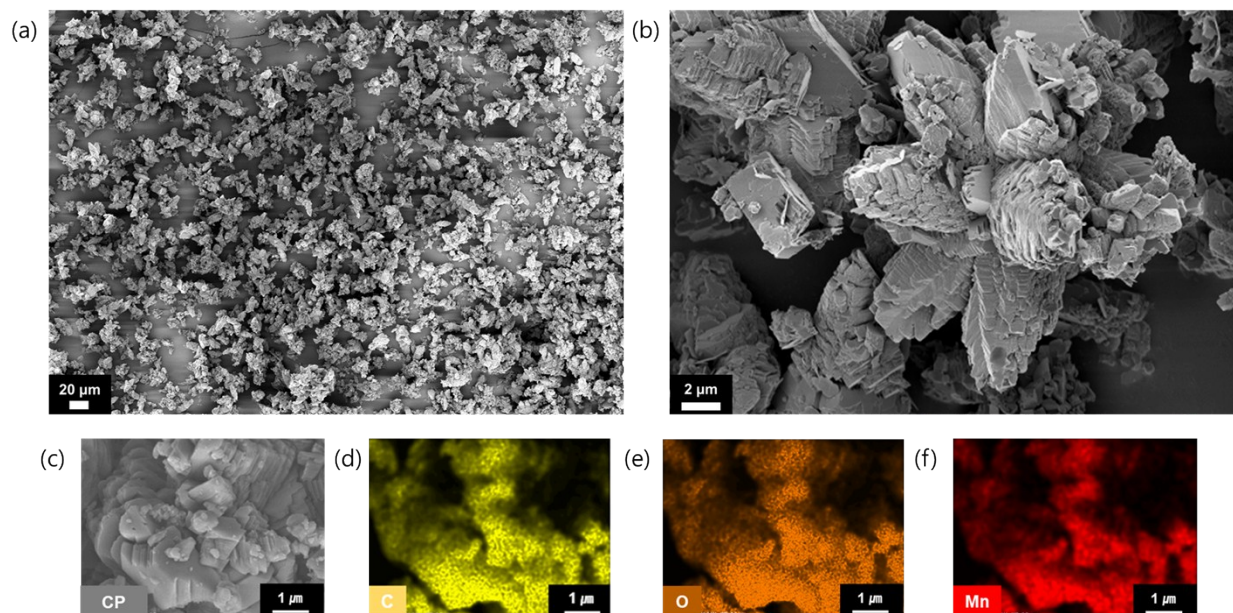


Fig. S2. (a) Low- and (b) high-magnification FESEM images of the Mn-CP. (c - f) Elemental mapping data displaying the distribution of C, O and Mn in Mn-CP

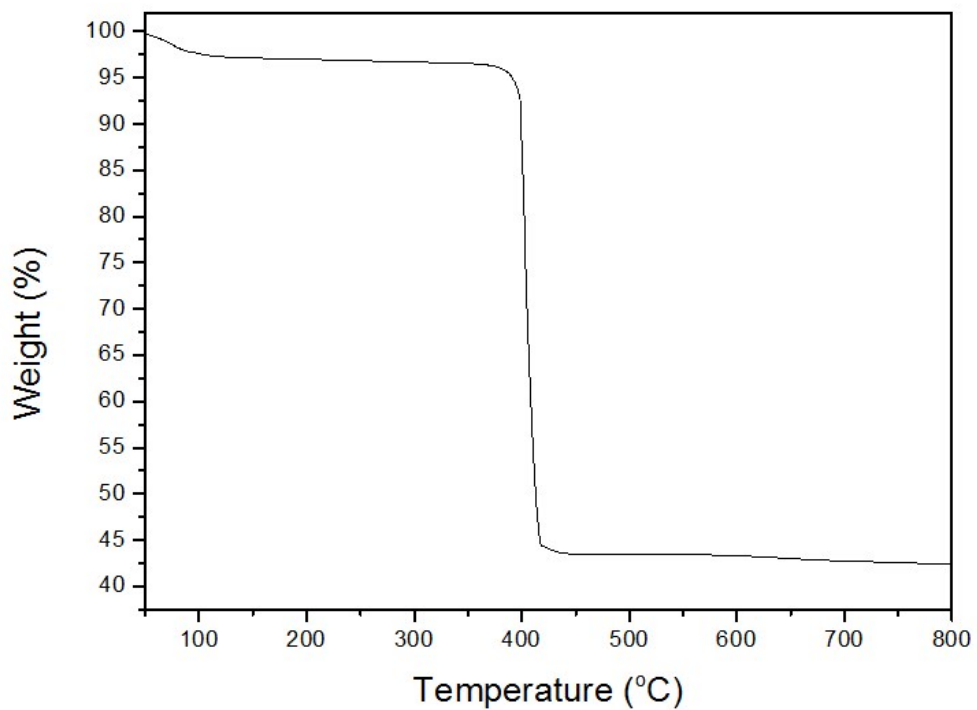


Fig. S3. TGA curve of Mn-CP.

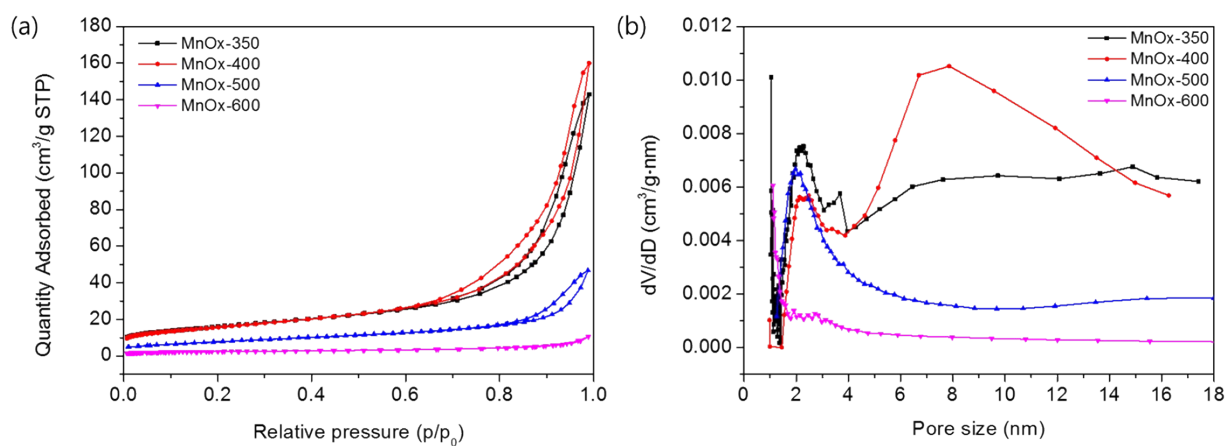


Fig. S4. (a) N₂ adsorption-desorption (BET isotherm) and (b) BJH pore size distribution of the MnOx catalysts.

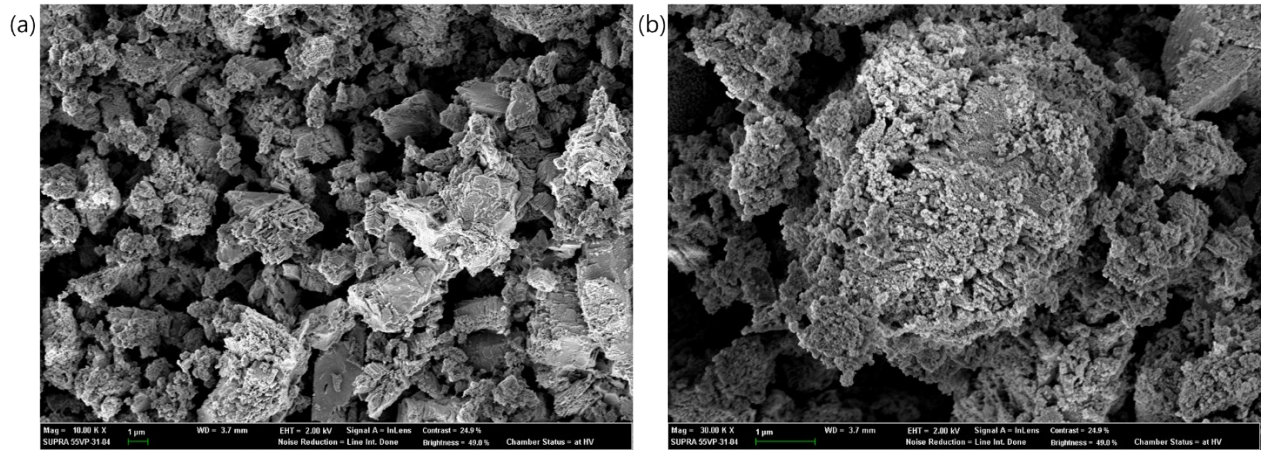


Fig. S5. (a) Low-magnification and (b) high-magnification FESEM images of MnOx-350 after catalytic reaction for 10 hours.

$$\frac{[400(\text{ppm})]_{in} - [34.8(\text{ppm})]_{out}}{[400(\text{ppm})]_{in}} \times 100(\%) = 91.3(\%) \quad (1)$$

$$\frac{[400(\text{ppm})]_{in} - [36(\text{ppm})]_{out}}{[400(\text{ppm})]_{in}} \times 100(\%) = 91(\%) \quad (2)$$

Equation S1. The catalytic conversion of NO_x using MnO_x-350 at (1) 150 °C and (2) 200 °C.

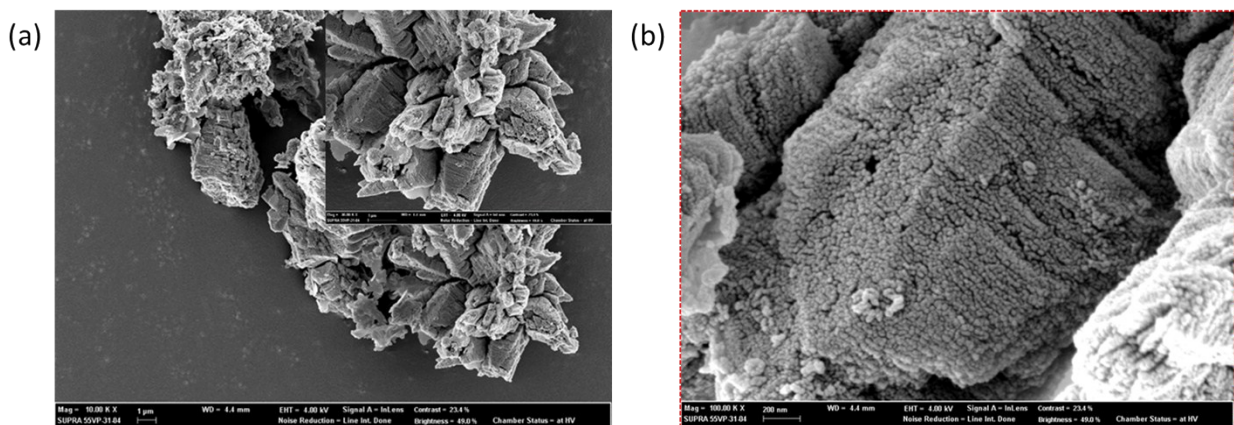


Fig. S6 SEM images of MnO_x-300

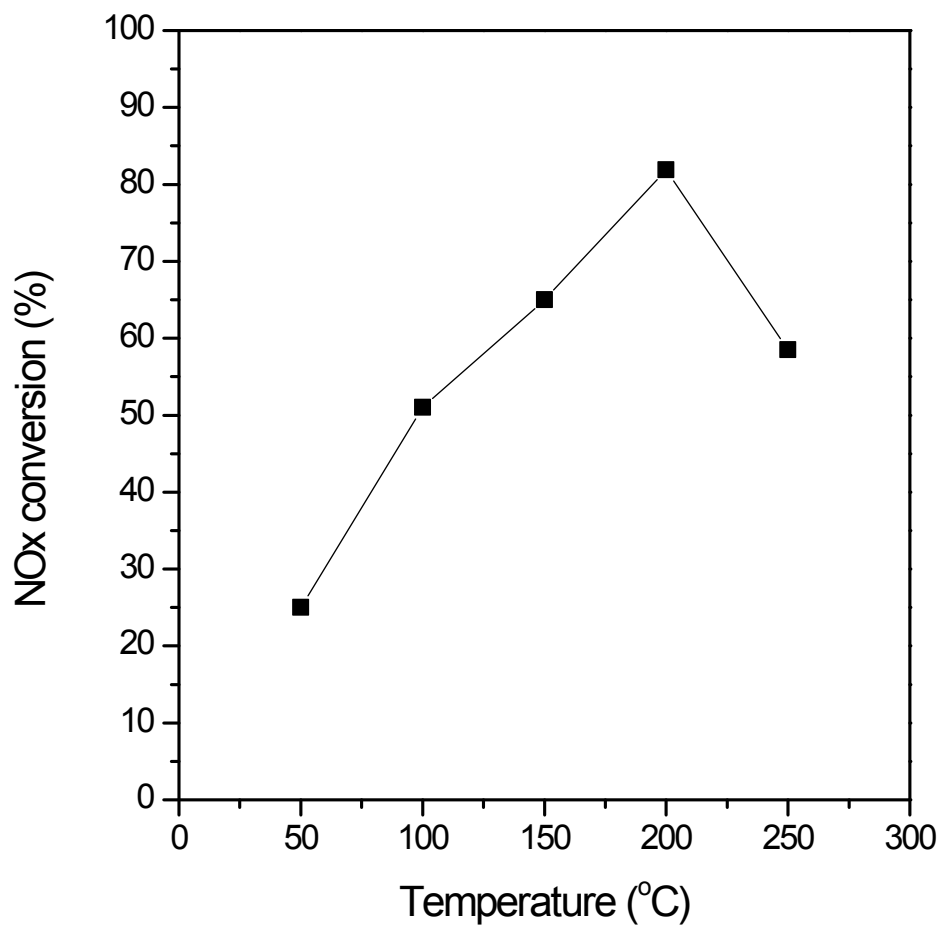


Fig. S7 NOx conversion efficiency of the MnOx-300

AUTHOR INFORMATION

Corresponding Author

sykwak@snu.ac.kr.